Ionic Dynamics in $LiNO_2$ Studied by ^7Li and ^{15}N Solid NMR

Hisashi Honda, Shin'ich Ishimaru[a], and Ryuichi Ikeda[a]

Faculty of Science, Yokohama City University, Kanazawa-ku, Yokohama 236-0027, Japan
[a] Department of Chemistry, University of Tsukuba, Tsukuba 305-8571, Japan

Reprint requests to Dr. H. H.; Fax: 81-45-787-2316; E-mail: hhonda@yokohama-cu.ac.jp

Z. Naturforsch. **54 a,** 519–523 (1999); received May 29, 1999

The temperature dependences of ^7Li and ^{15}N NMR spin-lattice relaxation times and spectra in $LiNO_2$ were measured in the range 120 K - 473 K (m.p.). The 180°-flip motion of NO_2^- ions along or perpendicular to the molecular C_2-axis and the self-diffusion of Li^+ ions (activation energies of 42 - 44 and 100 kJ mol^{-1}, respectively) were observed in this range. From the comparison of the observed activation parameters with those reported for plastic phases of alkali metal nitrites, a new characteristic of the plastic crystal was obtained.

Key words: ^7Li and ^{15}N Solid $LiNO_2$ NMR; Chemical Shift Anisotropy

Introduction

Nitrites of K, Rb, Cs, and Tl(I) become ionic plastic phases with NaCl- or CsCl-type cubic lattices around room temperature [1 - 4]. In the plastic phases, excitations of NO_2^- isotropic reorientation and self-diffusion were shown by the measurements of alkali metals and ^{15}N NMR [5 - 10]. In the low-temperature phase just below the plastic phase, the onset of two site flip motions of NO_2^- ions was observed [5 - 16].

$NaNO_2$, forming no plastic phase, undergoes two order-disorder phase transitions. The low-temperature phase is ferroelectric with all nitrite ions aligned parallel, and the middle phase is incommensurate(I) antiferroelectric with a sinusoidal modulation of the long-range order parameter [17 - 22]. In the high-temperature phase, a 180°-flip motion of NO_2^-, as observed in the low-temperature phases of K, Cs, and Tl salts [7, 9, 10], is excited about the axis perpendicular to the molecular C_2-axis [17 - 22].

In $LiNO_2$, no phase transition is reported between 80 and 473 K (melting point) [11]. The reported melting entropy of 36.2 J K^{-1} mol^{-1} is much larger than those in the plastic crystals: 14.0 (K), 16.0 (Rb), 17.8 (Cs), and 15.0 J K^{-1} mol^{-1} (Tl) [11 - 15], but comparable to 29.6 J K^{-1} mol^{-1} in $NaNO_2$ [23]. We are interested in the differences in the lattice dynamics of $LiNO_2$ from those of the other nitrites.

In the present study we have measured the temperature dependences of the ^7Li and ^{15}N NMR relaxation times and the spectra of $LiNO_2$, to reveal molecular motions in the wide temperature range of the solid phase and compare the observed activation parameters with those in the low-temperature-phases of the MNO_2 plastic crystals.

Experimental

$LiNO_2$ and ^{15}N enriched $Li^{15}NO_2$ were prepared from $NaNO_2$ (Wako Pure Chemical Industries Ltd.) and $Na^{15}NO_2$ (99wt% ^{15}N, ICON Inc.), respectively, by cation exchange using Diaion SK-1 obtained from Mitsubishi Kasei Corp. Crude crystals were recrystalized from ethanol and dried in vacuo at ca. 400 K for three days.

^7Li ($I = 3/2$) and ^{15}N ($I = 1/2$) NMR spectra and spin-lattice relaxation times T_1 were measured at the Larmor frequencies 116.64 and 30.42 MHz, respectively, with a Bruker MSL-300 spectrometer. ^7Li T_1 was also determined at 26 MHz using a Bruker SXP spectrometer. The saturation and inversion recovery methods were employed for evaluating T_1. ^{15}N spectra were recorded with an external reference of $^{15}NH_4^+$ ($\delta_s = -354$ ppm) in a 4.5 M solution of $^{15}NH_4NO_3$ in 3 M hydrochloric acid. ^7Li NMR spectra were obtained from FID signals observed after a $\pi/2$ pulse.

Since no crystal data are available, X-ray powder diffraction patterns were recorded at 300 and 440 K using a Philips X'Pert PW 3040/00 diffractometer with Cu anticathode. The electrical conductivity was

0932–0784 / 99 / 0800–0519 $ 06.00

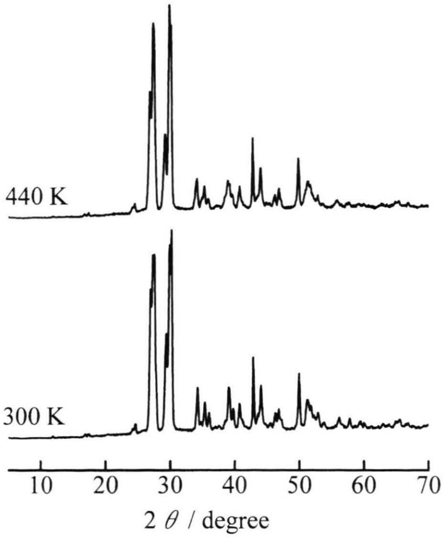

Fig. 1. X-Ray powder diffraction patterns observed in $LiNO_2$.

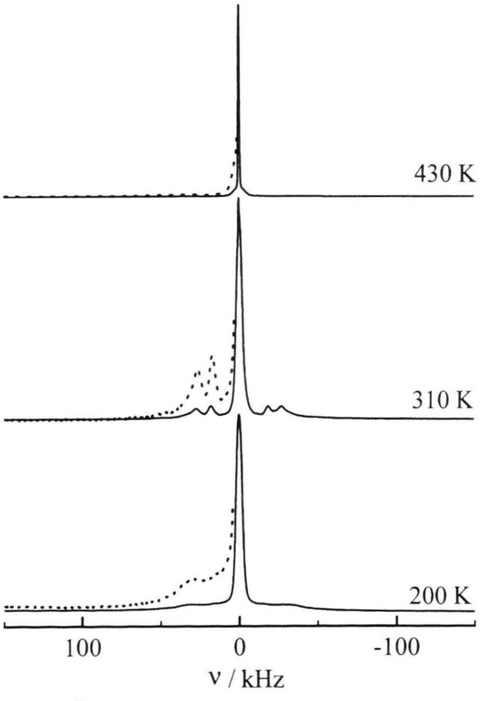

Fig. 2. ^{7}Li NMR powder spectra observed at 116.64 MHz in $LiNO_2$. The dotted spectra drawn on the left-hand side of the central peak are enlargements (×5).

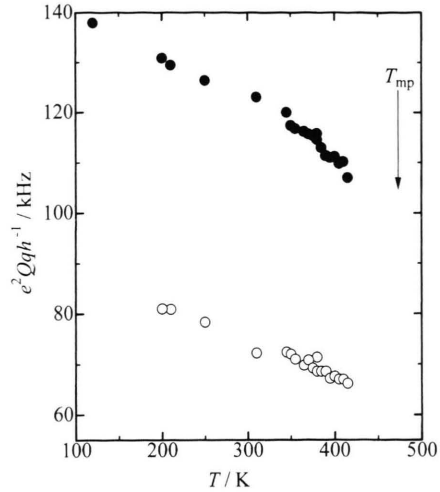

Fig. 3. Temperature dependences of ^{7}Li e^2Qqh^{-1}, estimated from the side-band width shown in Figure 2. The inner side band width at 120 K could not be determined because of the broadened central peak.

measured at 1 kHz with the two-terminal method using a Yokogawa Hewlett-Packard 4261A LCR meter at 350 - 470 K. The powdered sample was pressed into a disc, 1 cm in diameter and ca. 1 mm thick. Graphite electrodes (Acheson Electrodag 199) were employed.

Results and Discussion

X-Ray powder patterns recorded at 300 and 440 K are shown in Figure 1. These results suggest that $LiNO_2$ crystals retain a low symmetry up to the melting temperature.

Observed ^{7}Li NMR spectra measured at 116.64 MHz are shown in Figure 2. The satellites on both sides of the central peak imply the presence of two kinds of Li sites in the crystal. The quadrupole coupling constant e^2Qqh^{-1} of each ^{7}Li site was evaluated, assuming the asymmetry parameter $\eta = 0$, from the relation [24]

$$e^2Qqh^{-1} = 2\Delta\nu, \qquad (1)$$

where $\Delta\nu$ is the width between the satellite pair. The temperature dependence of observed e^2Qqh^{-1} is given in Figure 3. At room temperature we obtained e^2Qqh^{-1} values of (72±4) and (123±6) kHz, which decreased with increasing temperature, and a narrowed central peak was observed around 430 K after the satellites disappeared. Since our X-ray patterns showed no change around 430 K, it is expected

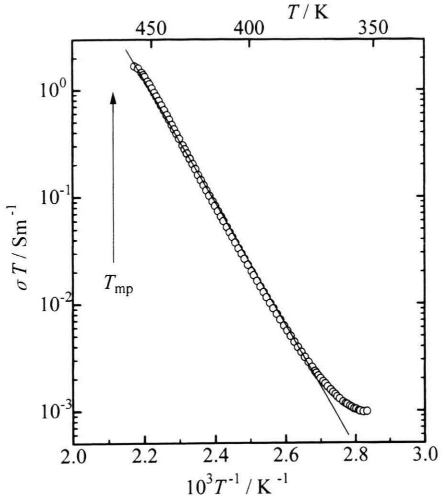

Fig. 4. The temperature dependence of the electrical conductivity σ of $LiNO_2$, measured at 1 kHz. The solid line gives an activation energy of 100± 5 kJ mol^{-1}. T_{mp} denotes the melting temperature.

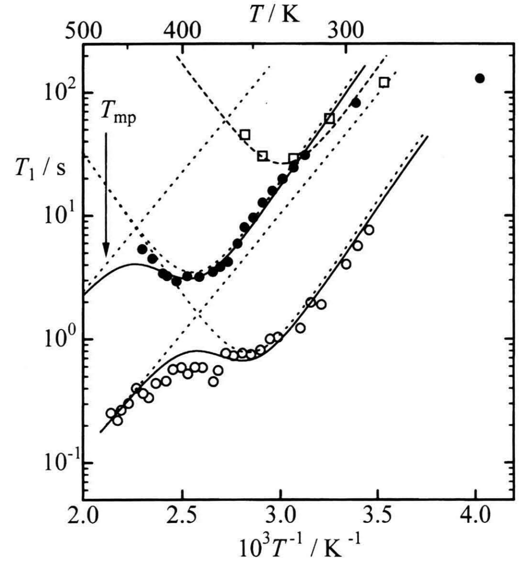

Fig. 5. Temperature dependences of T_1 of ^{7}Li observed at 116.64 (●) and 26 MHz (○) in $LiNO_2$, and of ^{15}N at 30.42 MHz (□) in $Li^{15}NO_2$. Solid, broken and dotted lines are the best fitted theoretical values. T_{mp} denotes the melting temperature.

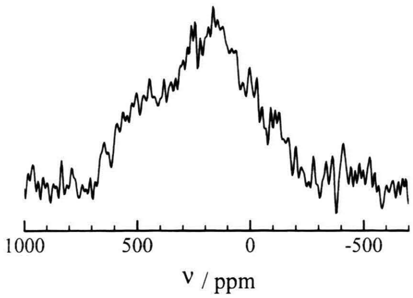

Fig. 6. An ^{15}N NMR powder spectrum observed at 30.42 MHz in $Li^{15}NO_2$ at 340 K.

that some ionic motions average the electric field gradient (EFG) at the Li$^+$ ions. As a possible motion we assumed cationic self-diffusion and carried out ac electrical conductivity measurements. The obtained temperature dependence of the electrical conductivity σ is shown in Figure 4. Upon heating to 460 K, σ increased to ca. 4×10^{-3} S m^{-1}, close to ca. 10^{-2} S m^{-1} reported in the plastic phase of MNO_2 (M = K, Rb, Cs, Tl) [7 - 10], suggesting that the conductivity is due to ionic conduction. Since σT is proportional to the diffusion coefficient, an activation energy of (100±5) kJ mol^{-1} was derived from the slope of log σT plotted against T^{-1}. This activation energy is almost equal to the 100 kJ mol^{-1} reported for KNO_2 [7] and $RbNO_2$ [8].

The temperature dependences of ^{7}Li T_1 observed at 116.64 and 26 MHz, and ^{15}N T_1 at 30.42 MHz are shown in Figure 5. ^{15}N T_1 gave a minimum around 330 K, explainable by the relaxation due to some motion. The ^{15}N NMR spectrum observed at 340 K, shown in Fig. 6, retains three different principal components of the chemical shift (CS) tensor which equal roughly those reported in the low-temperature phases of MNO_2 [7 - 10] and $NaNO_2$ [25, 26], where the NO_2^- 180°-flip was observed. Since the ^{15}N relaxation can be attributed mainly to the fluctuation of CS anisotropy, the observed T_1 is approximately expressed as [27]

$$\frac{1}{T_1} \approx \frac{3}{10}(\Delta\omega)^2\frac{\tau}{1+\omega_N^2\tau^2}, \qquad (2)$$

where $\Delta\omega$, ω_N, and τ denote the line-width narrowed by the CS averaging, the ^{15}N Larmor angular frequency, and the correlation time of the anionic motion, respectively. We assume an Arrhenius-type temperature dependence of τ given by

$$\tau = \tau_0 \exp\left(\frac{E_a}{RT}\right). \qquad (3)$$

Fitting (2) and (3) to the observed T_1 values, we obtained the best-fitted curve shown in Fig. 5 and an activation energy E_a of 42±5 kJ mol^{-1}. From the ^{15}N NMR spectrum with three different CS components observed even at 340 K and the temperature independent X-ray powdered patterns we suppose that the 180°-flip of the NO_2^- ion occurs about an axis along or perpendicular to the molecular C_2-axis, which can not cause marked changes in the NMR spectra, but contributes to the ^{15}N T_1. The motional mode of the NO_2^- 180°-flip about an axis perpendicular to the C_2-axis is acceptable in a low symmetry crystal structure because this mode was reported in the monoclinic structure ($P2_1/c$) phase of KNO_2 and explained by introducing an asymmetric double-minimum potential [16, 28].

A ^7Li T_1 minimum of ca. 3 s was observed at 116.64 MHz around 390 K, while T_1 at 26 MHz gave only a shoulder and decreased with increasing temperature above ca. 400 K, suggesting that two motional modes contribute to the ^7Li T_1. We tentatively expressed the observed T_1 by these relaxation times:

$$\frac{1}{T_1}=\frac{1}{T_{1L}}+\frac{1}{T_{1H}}. \qquad (4)$$

Here, T_{1L} and T_{1H} contribute in the low- and high-temperature ranges below and above ca. 400 K. As a relaxation mechanism, the fluctuation of the EFG at the ^7Li nuclei is most probable, and hence T_1 can be written by assuming the Debye-type spectrum density [27]

$$\frac{1}{T_1}=C\frac{\tau}{1+\omega_{Li}^2\tau^2}, \qquad (5)$$

where C, ω_{Li}, and τ denote a constant depending on the motional mode, the ^7Li Larmor angular frequency, and the correlation time of the motion, respectively. Since the slopes of ^7Li T_1 observed at (300 - 350) K were nearly equal to that of the ^{15}N T_1, the relaxation in this temperature range can be attributed to the 180°-flip of NO_2^- ions. Applying (3) and (5), the activation energy was determined to be (44±3) kJ mol^{-1}. On the other hand, the T_{1H} is attributable to the self-diffusion of Li^+ ions as confirmed by the ionic conductivity measurement. The activation energy of (40±10) kJ mol^{-1} estimated by using (3) and (5) is much smaller than 100 kJ mol^{-1}, evaluated from the electrical conductivity measurement. As possible reasons for this difference in E_a we can presume fitting errors in the E_a estimation from the ^7Li T_1 data due to too few experimental values in the high-temperature range, and also the assumption of the applicability of the BPP-type equation used for the analysis. Obtained motional modes and their activation energies are listed in Table 1.

Table 1. Motional modes, activation energies (E_a), and correlation times at infinite temperature (τ_0) determined from NMR and electrical conductivity measurements in $LiNO_2$.

Motional mode	E_a / kJ mol^{-1}	τ_0 / s	Method
NO_2^- 180°-Flip	42±5	1.3×10^{-15}	^{15}N T_1
	44±3	1.9×10^{-15}	^7Li T_1
Li^+ Self-diffusion	40±10	–	^7Li T_1
	100±5	–	electrical conductivity

Table 2. Comparisons in activation energies (E_a) of NO_2^- 180°-flip and cation self-diffusion in $M'NO_2$(M' = Li, K [7], Rb [8], Cs [10], and Tl [5, 6, 9]) determined by NMR. (Values in parenthesis are determined by electrical conductivity measurement.)

Motional mode	$LiNO_2$	KNO_2	$RbNO_2$	$CsNO_2$	$TlNO_2$
	— E_a / kJ mol^{-1} —				
180°-Flip	42 - 44	16.5 - 18.8	12 - 15*	8.7 - 11.7	14 - 17
Self-diffusion	40 (100)	60 (100)	75 - 140 (100)	33 - 47 (74)	47 (69)

* Energies are for the flip motion with a small angle about the anionic C_2-axis.

Conclusion

Li^+ self-diffusion and NO_2^- 180°-flip motion with activation energies of 100 and (42 - 44) kJ mol^{-1} were observed from the electrical conductivity and NMR measurements.

In the low-temperature phase of the plastic phases of MNO_2 (M = K, Cs, Tl) a 180°-flip of NO_2^- ions about an axis perpendicular to the C_2-axis was detected by dielectric relaxation and NMR studies [7, 9 - 10, 13 - 16]. The reported activation energies of (8.7 - 18.8) kJ mol^{-1} are much smaller than (42 - 44) kJ mol^{-1} in $LiNO_2$. On the other hand, the obtained correlation time of the 180°-flip at the melting point, $\tau_{mp} = 1.3\times10^{-10}$ s is close to the reported values of $\tau_{tr} \sim 1.0\times10^{-10}$ s in the plastic crystals MNO_2 [7 - 10], where τ_{tr} is the correlation time of the 180°-flip at the phase transition temperature to the plastic phase. These results suggest that, when the frequency of the 180°-flip motion reaches ca. 10 GHz, the phase transition takes place and an NO_2^- ion gets space for the isotropic reorientation. In the plastic phase, even if the isotropic reorientation of the NO_2^- ion is excited, the crystalline lattice is retained, while the $LiNO_2$ crystals become liquid. This difference can be explained by considering that the energies making spaces for the NO_2^- isotropic reorientation in MNO_2 are smaller than that in $LiNO_2$, as expected from the differences in energies of the 180°-flip motion in the low-temperature phases.

[1] J. K. Solbakk and K. O. Stromme, Acta. Chim. Scand. **23**, 300 (1969).
[2] P. W. Richter and C. W. F. T. Pisorius, J. Solid State Chem. **5**, 276 (1972).
[3] L. Cavalca, M. Nardelli, and I. W. Bassi, Gazz. Chim. Ital. **87**, 153 (1957).
[4] D. Hohlwein, A. Hoser, and W. Prandl, Z. Kristallogr. **177**, 93 (1986).
[5] Y. Furukawa and H. Kiriyama, Chem. Phys. Lett. **93**, 617 (1982).
[6] Y. Furukawa, H. Nagase, R. Ikeda, and D. Nakamura, Bull. Chem. Soc. Japan **64**, 3105 (1991).
[7] M. Kenmotsu, H. Honda, H. Ohki, R. Ikeda, T. Erata, A. Tasaki, and Y. Furukawa, Z. Naturforsch. **49a**, 247 (1994).
[8] H. Honda, M. Kenmotsu, H. Ohki, R. Ikeda, and Y. Furukawa, Ber. Bunsenges. Phys. Chem. **99**, 1009 (1995).
[9] H. Honda, S. Ishimaru, N. Onoda-Yamamuro, and R. Ikeda, Z. Naturforsch. **50a**, 871 (1995).
[10] H. Honda, M. Kenmotsu, N. Onoda-Yamamuro, H. Ohki, S. Ishimaru, R. Ikeda, and Y. Furukawa, Z. Naturforsch., **51a** 761 (1996).
[11] K. Moriya, T. Matsuo, and H. Suga, Thermochim. Acta **132**, 133 (1988).
[12] K. Moriya, T. Matsuo, and H. Suga, Bull. Chem. Soc. Japan **61**, 1911 (1988).
[13] K. Moriya, T. Matsuo, and H. Suga, Chem. Phys. Lett. **82**, 581 (1981).
[14] K. Moriya, T. Matsuo, H. Suga, and S. Seki, Chem. Lett. **1977**, 1427.
[15] K. Moriya, T. Matsuo, and H. Suga, J. Phys. Chem. Solids **44**, 1103 (1983).
[16] H. Honda, N. Onoda-Yamamuro, S. Ishimaru, R. Ikeda, S. Yamamuro, and T. Matsuo, Ber. Bunsenges. Phys. Chem. **102**, 148 (1998).
[17] A. Weiss, Z. Naturforsch. **15a** 536 (1960).
[18] Y. Takagi and K. Gesi, J. Phys. Soc. Japan **22**, 979 (1967).
[19] I. Hatta, J. Phys. Soc. Japan **24**, 1043 (1968).
[20] Y. Yamada, Y. Fujii, and I. Hatta, J. Phys. Soc. Japan **24**, 1053 (1968).
[21] R. Ikeda, M. Mikami, D. Nakamura, and M. Kubo, J. Magn. Reson. **1**, 211 (1969).
[22] T. Yagi, I. Tatsuzaki, and I. Todo, J. Phys. Soc. Japan **28**, 321 (1970).
[23] M. Sakiyama, A. Kimoto, and S. Seki, J. Phys. Soc. Japan **20**, 2180 (1965).
[24] M. H. Cohen and R. Reif, Solid State Phys. **5**, 321 (1957).
[25] R. E. Wasylishen, R. D. Curitis, K. Eichele, M. Lumsden, G. H. Penner, W. P. Power, and G. Wu, NATO ASI Ser. Ser. C **386**, 297 (1993).
[26] J. Moson, NATO ASI Ser. Ser. C **386**, 449 (1993).
[27] A. Abragam, The Principles of Nuclear Magnetism, Oxford University Press, London 1961.
[28] N. Onoda-Yamamuro, H. Honda, R. Ikeda, O Yamamuro, T. Matsuo, K. Oikawa, and F. Izumi, J. Phys. Condens. Matter **10**, 3341 (1998).